12th ICDERS, Ann Arbor, Michigan

July 23-28, 1989

Steady Deflagration Structure in Two-Phase Granular Propellants

Joseph M. Powers[1] ,

Mark E. Miller[2] , D. Scott Stewart[3] , and Herman Krier[4]

July 23-28, 1989

Abstract

This paper considers the rigorous formulation of a two-phase reactive flow model to describe steady deflagrations in reactive granular propellants. It is thought that granular propellants have the capability to provide significant gas generation and thus increased thrust in a rocket engine. It has been hypothesized that the normal operation of such an engine would consist of a constant velocity deflagration wave propagating through a mixture of propellant grains and gas. To predict the features of such a wave, steady deflagrations in granulated solid propellants have been studied using an improved two-phase reactive flow model. The improved model uses a time-dependent pore collapse equation to guarantee the unsteady one-dimensional equations are hyperbolic, conserves mass, momentum, and energy for the mixture, conserves the total number of particles, can accommodate density changes in the particles, and is capable of predicting steady detonations. At the point of complete reaction, an equivalent two-phase Rayleigh line and Hugoniot, independent of the wave structure, can be identified. As for one-phase systems, a maximum deflagration wave speed analogous to the one-phase Chapman-Jouguet (CJ) deflagration wave speed is found. By assuming the end state gas pressure is known and the reaction is complete, it is possible to fix the deflagration wave speed and gas phase end state. In the steady state, the model equations reduce to four ordinary differential equations. With this model, which does not consider gas phase heat conduction or radiative heat transport, no acceptable steady deflagration wave structure has been found. Based on this result, we speculate that deflagrations in a granulated propellant are likely accelerate to a detonation if a sufficient length of material is available and if sufficient confinement is maintained. It might be useful to test this theoretical result experimentally.

[1] Assistant Professor, Department of Aerospace and Mechanical Engineering, University of Notre Dame, Notre Dame, Indiana
[2] Member of Technical Staff, The Aerospace Corporation, El Segundo, California
[3] Associate Professor, Department of Theoretical and Applied Mechanics, University of Illinois at Urbana-Champaign, Urbana, Illinois
[4] Professor, Department of Mechanical and Industrial Engineering, University of Illinois at Urbana-Champaign, Urbana, Illinois; Fellow, AIAA

This work was performed with the support of the U.S. ONR, Contract N00014-86-K-0434, Dr. Richard S. Miller was Program Manager

Introduction

It is believed that steady deflagration of granulated solid propellants can increase the combustion wave speed and thrust when compared to the steady deflagration of cast propellants. A sketch of a hypothesized steady deflagration structure in a granulated propellant enclosed in a rocket engine casing is shown in Figure 1. It is hypothesized the solid propellant completely combusts to form a gas at a high pressure (10-100 MPa), subsonic state. The high pressure gas can then be expanded through a converging-diverging nozzle to atmospheric conditions, producing a thrust force.

It is generally thought that two-phase models have the ability to predict steady deflagrations in granulated propellants. Kuo, Summerfield and co-workers used two-phase theory to study steady deflagrations and unsteady flame front propagation in a series of papers in the mid 1970's [1,2,3,4]. The study of Ref. 3, which predicted steady deflagration in a mixture of mobile reactive particles and inert gas, is most relevant to the current study. In Ref. 3, a two-phase model is presented, Rankine-Hugoniot jump conditions are derived to describe the two-phase deflagration gas phase end state, and ordinary differential equations are integrated numerically to define the steady reaction zone structure. More recently Drew [5] has predicted steady deflagrations with a similar two-phase model, which unlike that of Ref. 3 considers gas phase heat conduction. In his study, several limits are taken so that it is possible to find an exact solution for the deflagration structure. The deflagration wave speed determined in Ref. 3 is dependent on the details of the gas phase conductive layer of the reaction zone structure.

In this paper, we study steady deflagrations in granulated propellants with a new two-phase model and describe the formulation of the two-phase deflagration problem. The model, similar to those of Refs. 3 and 5, is described in detail in Ref. 6 and has been used to predict two-phase detonation reaction zone structure in Ref. 7. The same two-phase detonation model can in principle be used to describe steady deflagrations. The model treats solid and gas phases as distinct entities. In addition to usual thermodynamic variables, the volume fraction is introduced

as a property of each phase. Separate mass, momentum, energy, and state equations are written for each phase. The phases are coupled through terms known as phase interaction terms. These terms represent mass, momentum, and energy transfer from one phase to another. The model is constructed such that the mass, momentum, or energy lost by one phase is transferred entirely to the other phase so that mixture mass, momentum, and energy are conserved.

The model of this study contains features which distinguish it from earlier two-phase deflagration studies. The model incorporates a dynamic pore collapse equation, first used by Baer and Nunziato in their studies of two-phase detonations [8]. The dynamic pore collapse equation is an evolutionary equation for volume fraction which holds that the volume fraction changes in response to differences in gas and solid stress states and chemical reaction. It is used in place of the algebraic equation relating gas and solid pressures used in Refs. 3 and 5. The algebraic equation holds that the gas and solid stresses equilibrate instantaneously. The dynamic pore collapse equation is controversial as there is no good experimental confirmation of its validity. Additional theoretical considerations suggest the equation's usefulness. Use of this equation guarantees the two-phase equations are hyperbolic, and thus well-posed for initial value problems. Also, as described in Refs. 6 and 7, the significance of the gas and solid sound speed and shock jumps is simplified when the dynamic compaction equation is used. Another distinguishing feature of this model is that it allows for a fully compressible solid. Although it is unlikely that solid compressibility effects are important in two-phase deflagrations, no significant complications are introduced by allowing the more general compressible solid. The gas phase equation of this study does not include heat conduction or radiation.

In order to conserve energy of the mixture, the solid energy equation of Drew and this study differs significantly from that of Kuo and Summerfield. In this study and Ref. 5, a solid energy equation is written which mirrors the form of the gas energy equation. The energy equations are written such that the principle of mixture energy conservation is satisfied. In the model formulation it is assumed that many particles exist within an averaging volume so that it

is possible to define an average particle temperature. This approach avoids the complications of a detailed consideration of individual particle-gas interactions. Thus with this approach it is impossible to determine the variation of particle temperature with radius. It is important to know the particle surface temperature when determining ignition and heat transfer. Because of this Kuo and Summerfield write a solid energy equation which allows the temperature profile of individual particles to be determined. They allow for heat conduction within the solid spherical particles. Their equation does not, however, insure that mixture energy is conserved. At this point we see no clear way to simultaneously achieve the goals of conserving mixture energy and determining detailed particle temperature profiles. Thus in this study, we have sacrificed knowledge of the temperature profiles in favor of a more fundamental principle, conservation of mixture energy.

The plan of this paper is as follows. A brief presentation is given of the steady two-phase model equations. Initial conditions for these equations are then discussed. Next the Rankine-Hugoniot deflagration jump conditions and Chapman-Jouguet (CJ) two-phase deflagration state is discussed. This discussion is similar to Powers, Stewart, and Krier's discussion of two-phase detonation end states [9] and Kuo and Summerfield's discussion of two-phase deflagration end states [3]. Unlike Ref. 3 the determination of deflagration gas phase end states and the initial conditions does not depend on the structure of the reaction zone. Finally, deflagration structure is considered. *In this study no acceptable deflagration structure was found.* In all cases considered, a singular point was reached in the structure. In the case presented here, the gas temperature approached absolute zero and gas density approached positive infinity at a point of incomplete reaction within the structure; thus, the structure is non-physical.

In searching for a steady two-phase deflagration, a wide variety of parameter space was sampled. That is to say, parameters such as the heat transfer and drag coefficients, equation of state parameters, compaction viscosity, etc. were varied. Because of the large number of parameters in the problem, the parametric study performed was incomplete. Part of the

parameter space tested is appropriate for describing common propellants, while other parts do not describe known propellants. While in no case was a structure found, some cases proved easier to resolve numerically. In order to clearly demonstrate a fully resolved deflagration structure whose gas phase properties became singular at a point of incomplete reaction, it was necessary to arbitrarily choose numerical values for some parameters. In this study, the solid state parameter σ, the compaction viscosity μ_c were chosen primarily so that a resolved structure could be presented. As a main purpose of this paper is to demonstrate the proper technique for this class of two-phase models, we believe there is value in using some numerical parameters which may be unrealistic if this allows the method to be more clearly illustrated.

MODEL EQUATIONS AND INITIAL CONDITIONS

The model equations are taken from Ref. 6. The solid mass, momentum, and energy equations are:

$$\frac{d}{d\xi}\left(\rho_2\phi_2 v_2\right) = -\left(\frac{3}{r}\right)\rho_2\phi_2\alpha P_1^m H(T_2 - T_{ig}), \tag{1}$$

$$\rho_2\phi_2 v_2\frac{dv_2}{d\xi} + \frac{d}{d\xi}\left[P_2\phi_2\right] = -\beta\frac{\phi_1\phi_2}{r}\left[v_2 - v_1\right], \tag{2}$$

$$\rho_2 v_2\frac{de_2}{d\xi} + P_2\frac{dv_2}{d\xi} = -h\frac{\phi_1}{r^{1/3}}\left[T_2 - T_1\right]. \tag{3}$$

In these equations, the subscripts "1" and "2" denote the gas and solid phase, respectively. The equations are written in the steady wave frame where $\xi = x - Dt$ is a distance in the wave frame and D is the steady wave speed. The velocity v is measured in the wave frame. Velocities in the lab frame,u, are given by $u = v + D$. The variable ρ represents the material density, that is

the mass of an individual phase divided by the volume occupied by that phase. The variable ϕ represents the volume fraction of each phase, that is the volume of an individual phase divided by the total volume. Pressure is denoted by P, internal energy by e, temperature by T, and particle radius by r. The constants α and m are empirical combustion model constants; β is an interphase drag constant, and h is an interphase heat transfer constant. The right sides of Equations (1), (2), and (3) are forcing functions representing interphase mass transfer, interphase drag, and interphase heat transfer, respectively. A Heaviside step function, H(x), appears in the mass transfer function to prevent mass transfer from occurring until the solid reaches a specified ignition temperature, T_{ig}.

The dynamic pore collapse equation is given by

$$v_2 \frac{d\phi_2}{d\xi} = \frac{\phi_1 \phi_2}{\mu_c}\left(P_2 - P_1 - \frac{P_{20} - P_{10}}{\phi_{20}}\phi_2\right) - \left(\frac{3}{r}\right)\phi_2 \alpha P_1^m H(T_2 - T_{ig}). \qquad (4)$$

Here μ_c is the compaction viscosity, a constant. No good experimental estimate of μ_c exists, and its value is a modeling assumption.

Conservation of mixture mass, momentum, and energy are given by

$$\rho_1\phi_1 v_1 + \rho_2\phi_2 v_2 = -D\,\rho_a, \qquad (5)$$

$$\rho_1\phi_1 v_1^2 + P_1\phi_1 + \rho_2\phi_2 v_2^2 + P_2\phi_2 = \rho_a D^2 + P_a, \qquad (6)$$

$$\rho_1\phi_1 v_1\left[e_1 + v_1^2/2 + P_1/\rho_1\right] + \rho_2\phi_2 v_2\left[e_2 + v_2^2/2 + P_2/\rho_2\right] = -\rho_a D\left[e_a + D^2/2 + P_a/\rho_a\right]. \qquad (7)$$

Here the subscript "a" denotes an apparent mixture property. The constants ρ_a, P_a, and e_a represent the initial mixture density, pressure, and energy, respectively. They are defined by the following equations:

$$\rho_a = \rho_{10}\phi_{10} + \rho_{20}\phi_{20}, \tag{8}$$

$$P_a = P_{10}\phi_{10} + P_{20}\phi_{20}, \tag{9}$$

$$e_a = \frac{\rho_{10}\phi_{10}e_{10} + \rho_{20}\phi_{20}e_{20}}{\rho_{10}\phi_{10} + \rho_{20}\phi_{20}}. \tag{10}$$

Here the subscript "0" denotes the initial condition. Number conservation implies the following expression for particle radius:

$$r = r_0 \sqrt[3]{\frac{-v_2\phi_2}{D\phi_{20}}}. \tag{11}$$

The gas phase is described by a virial state equation. Expressions for the thermal and caloric state equations are

$$P_1 = \rho_1 R T_1 \left(1 + b\rho_1\right), \tag{12}$$

$$e_1 = c_{v1} T_1. \tag{13}$$

Here R is the gas constant, b the virial coefficient, and c_{v1} the specific heat at constant volume. The solid phase is described by a Tait equation of state. The thermal and caloric state equations are given by

$$P_2 = \left(\gamma_2 - 1\right) c_{v2}\rho_2 T_2 - \frac{\rho_{20}\sigma}{\gamma_2}, \tag{14}$$

$$e_2 = c_{v2}T_2 + \frac{\rho_{20}\sigma}{\gamma_2\rho_2} + q. \tag{15}$$

Here γ_2 and σ are parameters in the Tait equation which can be fixed by matching experimental shock and compaction data. The constants c_{v2} and q are the solid specific heat at constant volume and chemical energy respectively. The mixture is constrained to be saturated so that

$$\phi_1 + \phi_2 = 1. \tag{16}$$

Equations (1-7) and (11-16) constitute a complete set of thirteen differential-algebraic equations for the thirteen unknowns, ρ_1, ρ_2, ϕ_1, ϕ_2, v_1, v_2, P_1, P_2, e_1, e_2, T_1, T_2, and r. In Ref. 7 it is shown how these equations can be written as four ordinary differential equations in four unknowns, ρ_2, ϕ_2, v_2, and P_2. This is accomplished by using the algebraic relations (5-7), (11-16) to write all remaining variables as functions of ρ_2, ϕ_2, v_2, and P_2.

We take as a modeling principle that in the undisturbed state, initial conditions for all variables are known, are consistent with the algebraic constraints, and are specified such that the undisturbed state is in equilibrium. At the initial state, one is allowed to specify eight initial conditions: the volume fraction of one phase, two thermodynamic variables for each phase (e.g. density and temperature), the velocity of each phase, and the initial particle radius. This is because in its original form the steady state is described by eight ordinary differential equations: two mass equations, two momentum equations, two energy equations, the dynamic pore collapse equation, and the number conservation equation. With a specified volume fraction, the saturation condition (16) fixes the remaining volume fraction. With a specified temperature and density for each phase, the state equations (12-15) fix the internal energy and pressure of each phase. To insure the initial state is an equilibrium state, it is specified that the initial solid temperature is below the ignition temperature to prevent mass transfer, the initial solid and gas

velocities are equal to prevent drag, and the initial solid and gas temperatures are equal to prevent heat transfer. The compaction equation has been constructed such that for $T < T_{ig}$, the initial state is an equilibrium state. Eight initial conditions for the original eight ordinary differential equations are given in Equations (17-18):

$$\rho_2 = \rho_{20}, \quad \phi_2 = \phi_{20}, \quad v_2 = -D, \quad T_2 = T_0. \tag{17}$$

$$\rho_1 = \rho_{10}, \quad v_1 = -D, \quad T_1 = T_0, \quad r = r_0. \tag{18}$$

The remaining initial conditions are specified such they are consistent with the state equations and saturation condition:

$$P_{10} = \rho_{10} R T_0 \left(1 + b\rho_{10}\right), \quad e_{10} = c_{v1} T_0,$$

$$P_{20} = \left(\gamma_2 - 1\right) c_{v2} \rho_{20} T_0 - \frac{\rho_{20}\sigma}{\gamma_2}, \quad e_{20} = c_{v2} T_0 + \frac{\sigma}{\gamma_2} + q,$$

$$\phi_{10} = 1 - \phi_{20}. \tag{19}$$

The initial conditions specified in Equations (17-19) are used in determining the integration constants in the integrated mixture and number conservation equations. Of the remaining four differential equations, which can be solved explicitly for the derivatives of ρ_2, ϕ_2, v_2, and P_2 in terms of ρ_2, ϕ_2, v_2, and P_2, the above initial conditions contain the appropriate initial values.

The frozen gas and solid sound speeds, a, which are thermodynamically consistent with the state equations are specified by the following equations:

$$a_1^2 = RT_1\left(1 + 2b\rho_1 + (R/c_{v1})(1 + b\rho_1)^2\right), \tag{20}$$

$$a_2^2 = \gamma_2 (\gamma_2 - 1) c_{v2} T_2. \tag{21}$$

Numerical values for parameters for the parameters of these equations are listed in Table I. The origin of some the values is discussed in detail in Ref. 7. Some are based on independent experimental observation, though some parameters, such as gas phase state constants have been chosen to force the detonation predictions of the theory match experimental detonation observations. Other parameters, such as the heat transfer coefficient, drag coefficient, are not known under detonation conditions and were estimated in Ref. 7 such that one could predict a detonation structure. In this study the compaction viscosity μ_c and solid state parameter σ were estimated so that a deflagration structure could be exhibited.

COMPLETE REACTION DEFLAGRATION GAS END STATES

It is assumed that the gas pressure at the end of the reaction zone can be controlled [3,5]. Here, it is shown how the deflagration wave speed and other end state properties are dependent on the gas pressure at the end of the reaction zone.

If it is hypothesized that the complete reaction state ($\phi_2 = r = 0$) is an equilibrium end state of the differential equations (1-4), then it is possible to use the mixture equations (5-7) to write two-phase equivalents to the Rayleigh line (22) and Hugoniot (23).

$$P_1 = P_a + \rho_a^2 D^2 \left(1/\rho_a - 1/\rho_1 \right), \tag{22}$$

$$\frac{(P_a + P_1)(1/\rho_1 - 1/\rho_a)}{2} + \frac{c_{v1} P_1}{R\rho_1 (b\rho_1 + 1)} - e_a = 0. \tag{23}$$

These equations are found by setting $\phi_2 = 0$ in the mixture equations. The mixture mass equation is used to eliminate v_1 in the mixture momentum equation to form the two-phase

Rayleigh line equation (22). This equation is a line in P_1, $1/\rho_1$ space with a negative slope proportional to the square of the wave speed. The two-phase Hugoniot (23) is found by using the gas state equations (12) and (13) to eliminate e_1 in favor of P_1 and ρ_1 in the mixture energy equation. Then v_1 can be eliminated with the mixture mass equation, and D can be eliminated with the Rayleigh line equation. What remains is an equation in terms of P_1 and $1/\rho_1$ and independent of velocity or wave speed.

The gas phase complete reaction end state is specified once a wave speed is chosen. The analysis is analogous to a one-phase end state analysis. For a given wave speed D, Equation (22) can be used to eliminate pressure in Equation (23) to form a cubic equation for final gas density. Once final density is determined, Equation (22) can be used to determine final pressure. Thus, the wave speed is known as a function of the final pressure. The mixture mass equation then can be used to fix the final gas velocity, and the state equations fix the final temperature and energy. One of the roots of the cubic density equation is nonphysical and is associated with the singularity in the Hugoniot at $1/\rho_1 = -b$. For the ideal gas $b = 0$, the density equation is quadratic, and the spurious root does not exist. Depending on the wave speed, the two remaining roots are real or imaginary.

At two specific wave speeds, the two physical roots are degenerate. This condition is known as the two-phase CJ condition. The lower of the CJ wave speeds is the CJ deflagration speed, D_{CJDEF}, and the higher is the CJ detonation speed, D_{CJDET}. For $D < D_{CJDEF}$, two physical end states exist, one whose velocity is supersonic relative to the wave head, known as a strong deflagration, and another whose velocity is subsonic relative to the wave head, known as a weak deflagration. For $D = D_{CJDEF}$, the two roots are degenerate; a single physical end state exists whose velocity is sonic with respect to the wave head. For $D_{CJDEF} < D < D_{CJDET}$, two imaginary roots exist and no physical end state exists. For $D = D_{CJDET}$, the two real roots are degenerate, and again a single physical end state exists whose velocity is sonic relative to the wave head. For $D > D_{CJDET}$, two real roots exist. A supersonic final velocity is associated

with one root, known as the weak detonation solution. A subsonic final velocity is associated with the other, known as the strong detonation solution.

At the two-phase CJ deflagration or detonation state, the two-phase Rayleigh line is tangent to the two-phase Hugoniot. One way to determine this state is to enforce the tangency condition:

$$\left.\frac{dP_1}{d\rho_1}\right|_{\text{Equation 22}} = \left.\frac{dP_1}{d\rho_1}\right|_{\text{Equation 23}} \tag{24}$$

For the ideal gas, b = 0, it is possible to determine an analytic expression for the CJ deflagration and detonation velocity by solving Equations (22-24) simultaneously. The solution is

$$D_{CJ}^2 = \frac{(2c_{v1}+R)\,Re_a - c_{v1}^2 P_a/\rho_a \pm \sqrt{(2c_{v1}+R)\left(e_a^2 R^2 (2c_{v1}+R) - (2e_a+P_a/\rho_a)c_{v1}^2 P_a R/\rho_a\right)}}{c_{v1}^2} \tag{25}$$

Here the minus branch of this equation corresponds to the CJ deflagration state and the plus branch corresponds to the CJ detonation state. When the dimensionless group $P_a/(\rho_a e_a) << 1$, the CJ deflagration state simplifies considerably. In this limit, which is relevant for many physical systems, the CJ deflagration state is approximated by the following equations:

$$D_{CJ} \cong \sqrt{\frac{\gamma_1^2 e_a}{2(\gamma_1^2 - 1)}}\left(\frac{P_a}{\rho_a e_a}\right), \tag{26}$$

$$P_{CJ} \cong \frac{1}{\gamma_1 + 1} P_a, \tag{27}$$

$$\rho_{CJ} \cong \frac{\gamma_1}{2(\gamma_1 - 1)}\left(\frac{P_a}{\rho_a e_a}\right)\rho_a, \tag{28}$$

$$T_{CJ} \cong \frac{2}{\gamma_1 (\gamma_1 + 1)}\frac{e_a}{c_{v1}}, \tag{29}$$

$$e_{CJ} \cong \frac{2}{\gamma_1(\gamma_1 + 1)}e_a, \tag{30}$$

$$v_{CJ} \cong u_{CJ} \cong -\sqrt{\left(\frac{2(\gamma_1 - 1)}{\gamma_1 + 1}e_a\right)}\ . \tag{31}$$

Here $\gamma_1 = 1 + R/c_{v1}$ and is equivalent to the ratio of specific heats for an ideal gas.

A sketch of the two-phase Rayleigh line and Hugoniot is shown in Figure 2. Potential end states exist at the where the Rayleigh line intersects the Hugoniot. For $D < D_{CJDEF}$, the figure shows the strong and weak solutions, and for $D = D_{CJDEF}$, the CJ solution is shown. Also shown for both cases are the nonphysical solutions ($1/\rho_1 < 0$).

It should be noted that the two-phase Rayleigh line and Hugoniot equations (and thus the sketch of Figure 2) are only valid at the complete reaction state. For incomplete reaction at a given $\phi_2 \neq 0$, the mixture equations define a surface in P_1, $1/\rho_1$, P_2, $1/\rho_2$ hyperspace. This is in contrast to one-phase theory where the Rayleigh line and Hugoniot can be represented in P, $1/\rho$ space throughout the reaction zone.

The CJ deflagration state has been determined exactly for $b \neq 0$ by a numerical trial and error approach using the approximate formulae (26-31) as a first guess. For the parameters of Table I, the CJ deflagration wave speed is plotted versus initial bulk density ρ_a in Figure 3. It is seen that the CJ deflagration wave speed rises as the initial bulk density decreases. For the conditions of Table I, and $\phi_{20} = 0.70$, Figures 4 and 5 show deflagration wave speed and lab frame final velocity as a function of final gas pressure. It is seen that for a given wave speed,

two final pressures are predicted, the lower pressure associated with the strong supersonic solution and the higher pressure associated with the weak subsonic solution.

TWO-PHASE DEFLAGRATION STRUCTURE

An analysis of the complete reaction state ($\phi_2 = r = 0$) is insufficient to describe two-phase deflagration structure. The analysis does limit deflagration wave speeds to speeds less than or equal to the CJ deflagration speed and given an end state gas pressure can predict a deflagration wave speed and remaining gas phase end state variables. The end state analysis does not prove, however, that the complete reaction state is an equilibrium point of the differential equations (1-4). Other equilibrium states at points of incomplete reaction may exist within the reaction zone structure. Furthermore, a steady structure analysis is necessary to determine if all variables within the reaction zone are physical.

It is arbitrarily assumed for this discussion that neither shock waves nor sonic points exist in the deflagration structure, though neither can be ruled out a priori. The analysis becomes significantly more complicated if such conditions exist. Two-phase shock jumps are usually associated with two-phase detonations and are considered in more detail in Ref. 7. In the analysis of this study and Ref. 7, which does not consider diffusive processes, shock jumps are discontinuous jumps in pressure, velocity, etc., and are specified by algebraic equations. The shock discontinuity equations specify the shocked state as a function of wave speed and the unshocked state. In principle a shock in either phase could exist at any point within the deflagration structure. At sonic points or points where either the gas velocity equals the local gas sound speed or the solid velocity equals the local solid sound speed, the two-phase differential equations are singular, [7] which significantly complicates the analysis.

With the assumption of no shocks or sonic points in the structure, if the deflagration wave speed is less than the ambient gas sound speed, the entire deflagration structure is subsonic. If a complete reaction point is reached, it is at the weak solution point. If the deflagration wave

speed is greater than the ambient gas sound speed, then the entire deflagration structure is supersonic. If a complete reaction point is reached, it is at the strong solution point. For the parameters of Table I, the ambient gas sound speed is 589 m/s. Except in the dilute limit ($\phi_{20} \sim 0$), this speed is greater than the CJ deflagration speed. Thus for a wide range of initial solid volume fractions, the solution is subsonic and drawn to the weak point. Consequently Figure 4 indicates that the final pressure must be on the order of of thousands of atmospheres.

The structure analysis proceeds as follows. Initial conditions for v_{20} (= wave speed, -D), ρ_{20}, ϕ_{20}, and P_{20} are fixed at $\xi \geq 0$. In this analysis it is assumed that the ignition temperature is arbitrarily close to the ignition temperature, so that combustion begins at $\xi = 0$. The ordinary differential equations are then integrated with respect to ξ in the direction of negative ξ. The integration is continued until either an equilibrium end state is reached or a nonphysical point in the reaction zone structure is found. The integration was performed using the IMSL subroutine DIVPRK, a fifth and sixth order Runge-Kutta-Verner routine, on the UIUC Convex digital computer. Run times were less than one minute.

For the conditions of Table I, with $\phi_{20} = 0.70$ and D = 100 m/s ($< D_{CJDEF} = 135$ m/s), a deflagration structure has been calculated up to the point where the structure became nonphysical. Figures 6-11 show gas and solid density, solid volume fraction, gas and solid lab frame velocity, gas and solid pressure, gas and solid temperature, and gas and solid Mach number squared ($M^2 = v^2/a^2$), respectively, versus distance. From these figures, it is seen that at a point about 10 mm within the reaction zone structure, the gas density approaches positive infinity, the gas temperature approaches absolute zero, the gas Mach number approaches zero, and the reaction is incomplete ($\phi_2 = 0.686$). The gas phase Mach number approaches zero, because the wave frame gas velocity v_1 approaches zero faster than the gas sound speed which also approaches zero. On the scales shown in Figures 6-11, the change in solid variables is not apparent; however, there is a small variation in solid variables within the structure. There is a small scale variation in gas phase variables near $\xi = 0$ which is not fully resolved in Figures 6-11. This variation, which can be fully resolved is not important for the present discussion.

In Ref. 7 it is shown how in the limit of infinite compaction viscosity and zero heat transfer, the two-phase reaction zone structure can be reduced to solving two differential equations in two unknowns. This two equation model proved useful in analyzing two-phase detonations as it allows two-dimensional phase portraits to be generated. The two-equation model was also used to study deflagrations. As for the full model equations, no deflagration structure was found which reached complete reaction.

DISCUSSION

This study suggests, but does not prove, that for the class of two-phase models studied steady two-phase deflagrations do not exist. Since the same model is able to predict a steady two-phase detonation, this suggests that a transient study of the two-phase model could show that combustion phenomena in granular propellants tend to accelerate to detonations. An alternate conclusion is that steady deflagrations may exist, but that this particular model is incapable of describing one. The results indicate that the mechanisms of interphase heat transfer, interphase drag, compaction, and chemical reaction which are sufficient to support a steady two-phase ~~deflagration~~ detonation are not sufficient to support a two-phase deflagration. It may be necessary to include diffusive mechanisms of energy and momentum transport in order describe a steady deflagration.

The failure to predict a steady deflagration does not necessarily mean that granular propellants have no utility in rocket propulsion. It is possible that the combustion of granular propellants is an inherently unsteady process. An unsteady analysis of the two-phase equations could identify if the unsteady wave speed in a granular propellant is indeed faster than the steady wave speed in an equivalent cast propellant. Such an analysis would also indicate whether the unsteady combustion wave accelerates to a detonation wave and the length scale required to reach a detonation. Thus one could determine whether or not granular propellants were feasible for rocket propulsion.

REFERENCES

[1] Kuo, K. K., Vichnevetsky, R., and Summerfield, M., 1973, "Theory of Flame Front Propagation in Porous Propellant Charges under Confinement," *AIAA J.* **11**, 444-451.

[2] Kuo, K. K., and Summerfield, M., 1974, "Theory of Steady-State Burning of Gas-Permeable Propellants," *AIAA J.* **12**, 49-56.

[3] Kuo, K. K., and Summerfield, M., 1975, "High Speed Combustion of Mobile Granular Solid Propellants: Wave Structure and the Equivalent Rankine-Hugoniot Relation," in Fifteenth *Symposium (International) on Combustion*, The Combustion Institute, Pittsburgh, PA, 515-527.

[4] Kuo, K. K., Koo, J. H., Davis, T. R., and Coates, G. R., 1976, "Transient Combustion in Mobile Gas-Permeable Propellants," *Acta Astronautica* **3**, 573-591.

[5] Drew, D. A., 1986, "One-Dimensional Burning Wave in a Bed of Monopropellant Particles," Combust. Sci. and Tech. **47**, 139-164.

[6] Powers, J. M., Stewart, D. S., and Krier, H., 1989, "Theory of Two-Phase Detonation--Part I Modeling," to appear in *Combust. Flame.*

[7] Powers, J. M., Stewart, D. S., and Krier, H., 1989, "Theory of Two-Phase Detonation--Part II Structure," to appear in *Combust. Flame.*

[8] Baer, M. R., and Nunziato, J. W., 1986, "A Two-Phase Mixture Theory for the Deflagration-to-Detonation Transition (DDT) in Reactive Granular Materials," *Int. J. Multiphase Flow* **12**, 861-889.

[9] Powers, J. M., Stewart, D. S., and Krier, H., 1988, "Two-Phase Steady Detonation Analysis," in Dynamics of Explosions (A. L. Kuhl, F. R. Bowen, J.-C. Leyer, and A. Borisov, Eds.) Vol. 114 of *Progress in Astronautics and Aeronautics*, AIAA, Washington, DC, 341-361.

Table I

DIMENSIONAL INPUT PARAMETERS

a	$[m / (s\ Pa)]$	2.90×10^{-9}
ρ_{10}	$[kg / m^3]$	1.00×10^{0}
m		1.00×10^{0}
β	$[kg / (s\ m^2)]$	1.00×10^{4}
ρ_{20}	$[kg / m^3]$	1.90×10^{3}
h	$[J / (s\ K\ m^{8/3})]$	1.00×10^{7}
c_{v1}	$[J / (kg\ K)]$	2.40×10^{3}
c_{v2}	$[J / (kg\ K)]$	1.50×10^{3}
R	$[J / (kg\ K)]$	8.50×10^{2}
σ	$[(m / s)^2]$	7.20×10^{6}
q	$[J / kg]$	5.84×10^{6}
r_0	$[m]$	1.00×10^{-4}
b	$[m^3 / kg]$	1.10×10^{-3}
γ_2		5.00×10^{0}
μ_c	$[kg / (m\ s)]$	1.25×10^{2}
T_0	$[K]$	3.00×10^{2}
T_{ig}	$[K]$	$3.00 \times 10^{2}+$

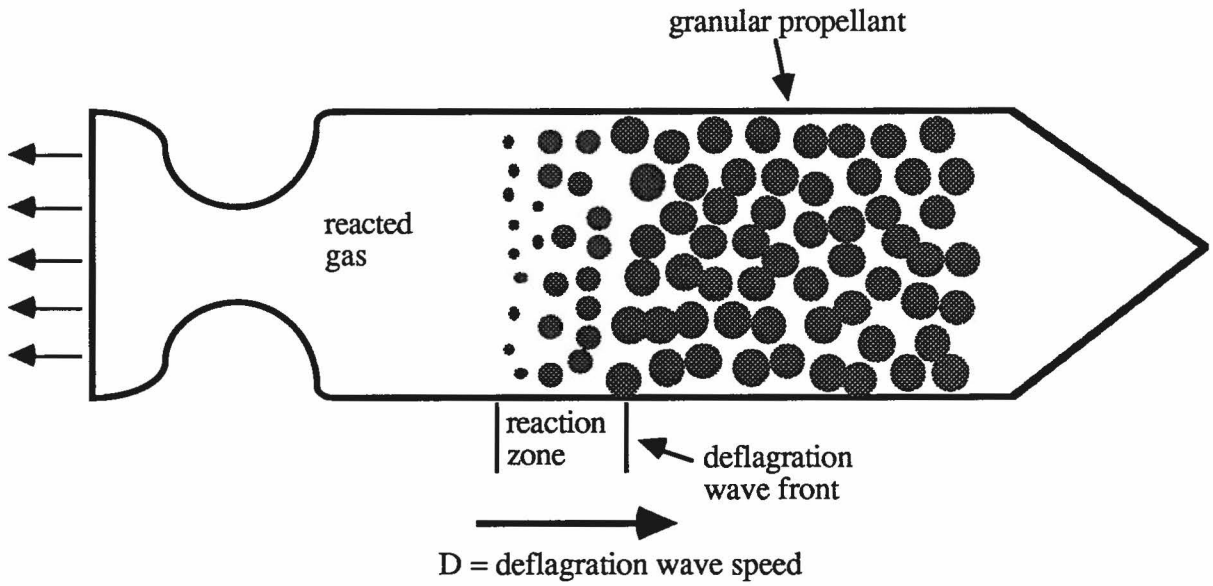

Figure 1 Sketch of Envisioned Steady Deflagration Structure in Rocket

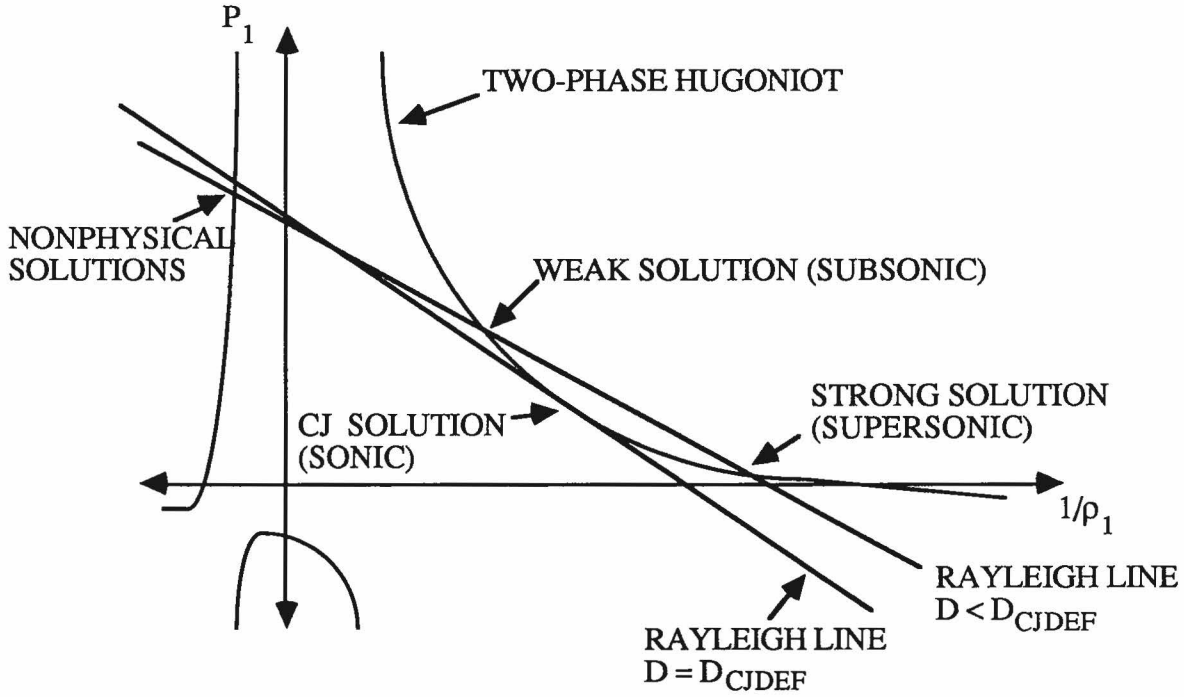

Figure 2 Two-Phase Complete Reaction Deflagration Rayleigh Line and Hugoniot

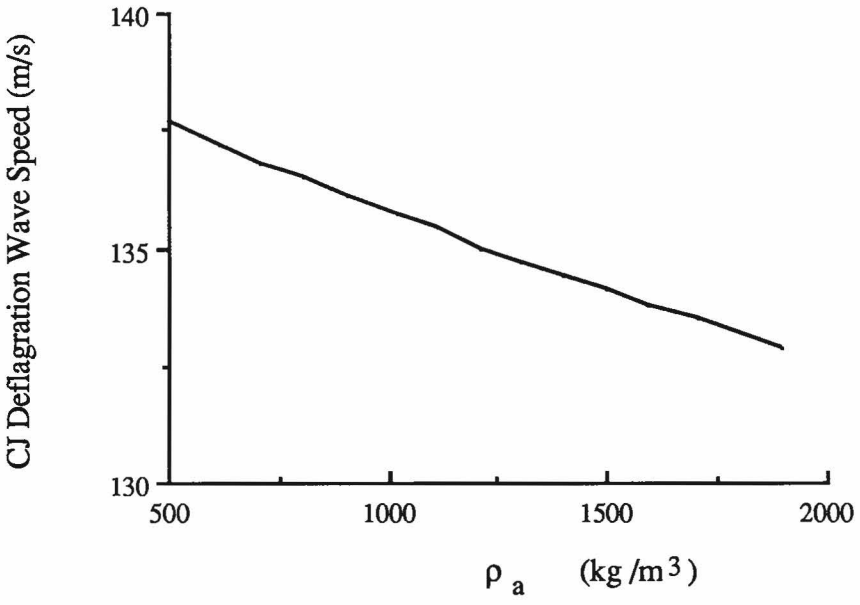

Figure 3 CJ (Maximum) Deflagration Wave Speed versus Initial Bulk Density

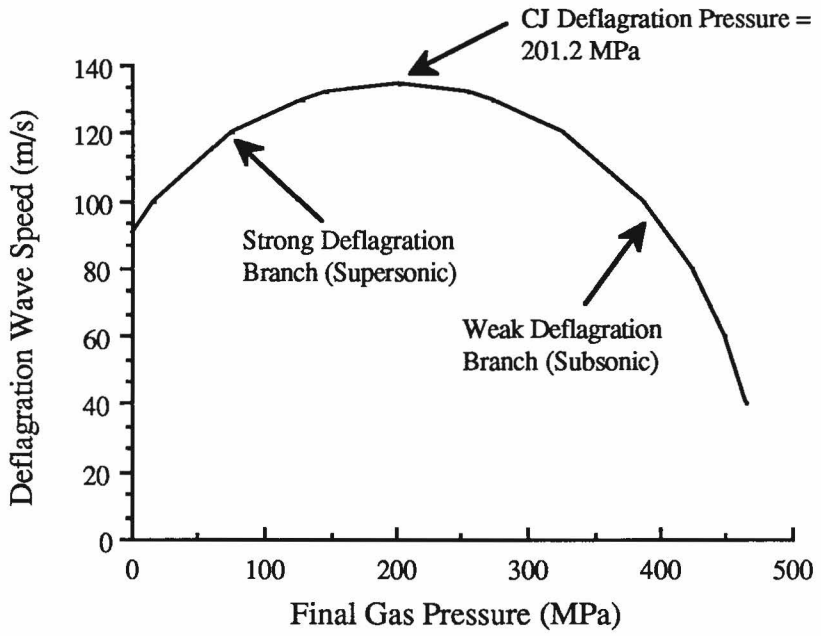

Figure 4 Deflagration Wave Speed versus Final Gas Pressure, $\phi_{20} = 0.70$

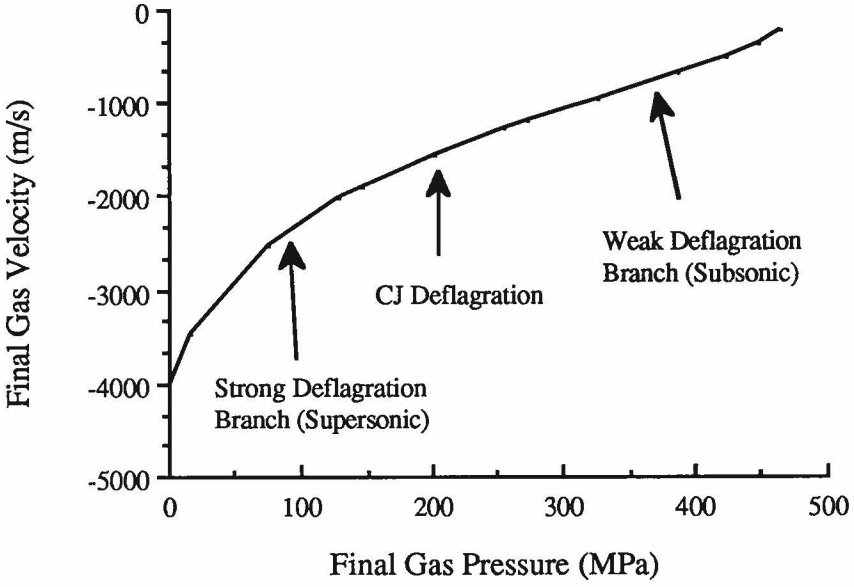

Figure 5 Final Lab Frame Gas Velocity versus Final Gas Pressure, $\phi_{20} = 0.70$

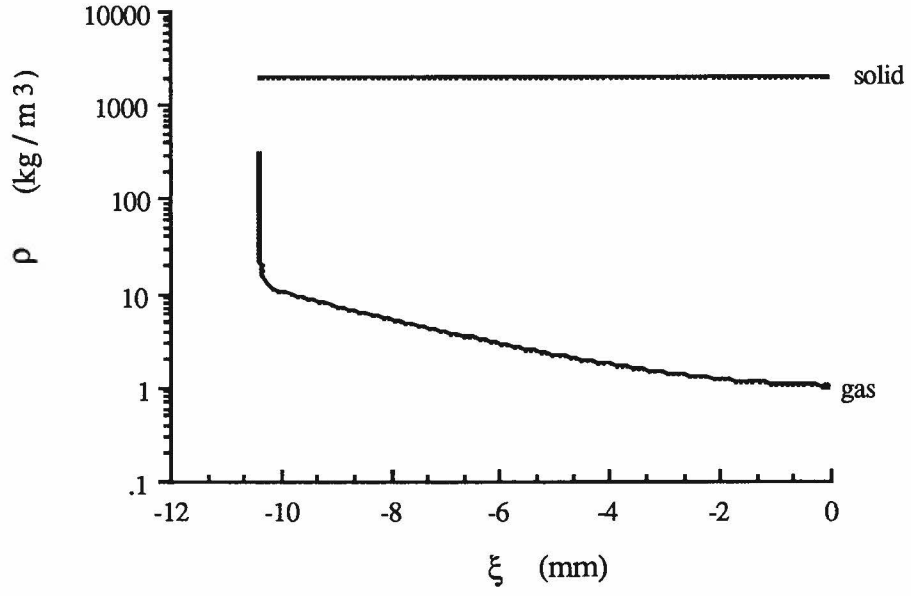

Figure 6 Gas and Solid Density Structure, $\phi_{20} = 0.70$, D = 100 m/s

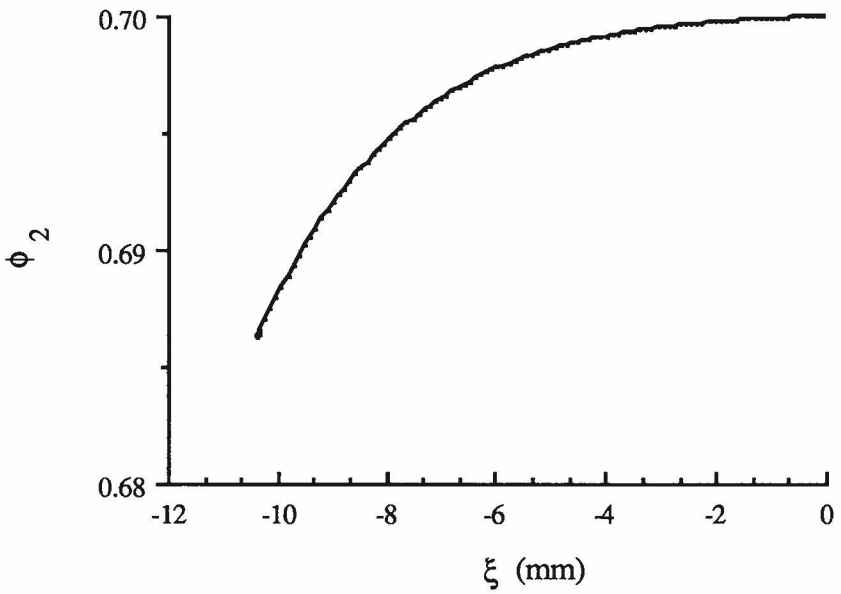

Figure 7 Solid Volume Fraction Structure, $\phi_{20} = 0.70$, D = 100 m/s

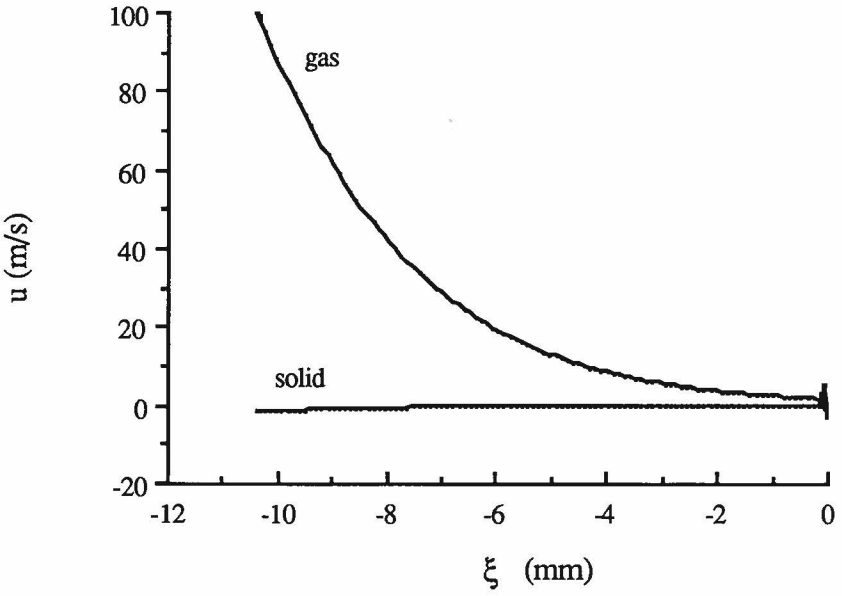

Figure 8 Gas and Solid Lab Velocity Structure, $\phi_{20} = 0.70$, D = 100 m/s

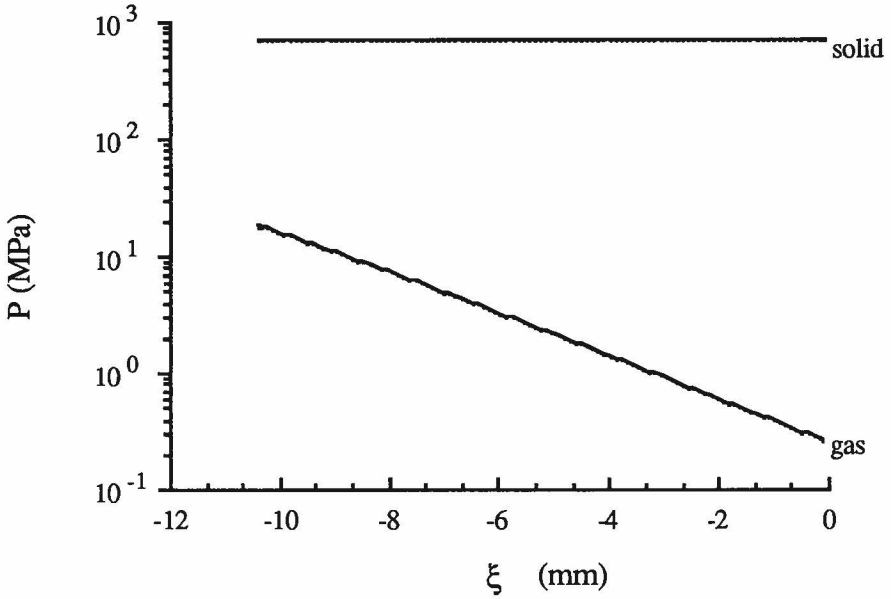

Figure 9 Gas and Solid Pressure Structure, ϕ_{20} = 0.70, D = 100 m/s

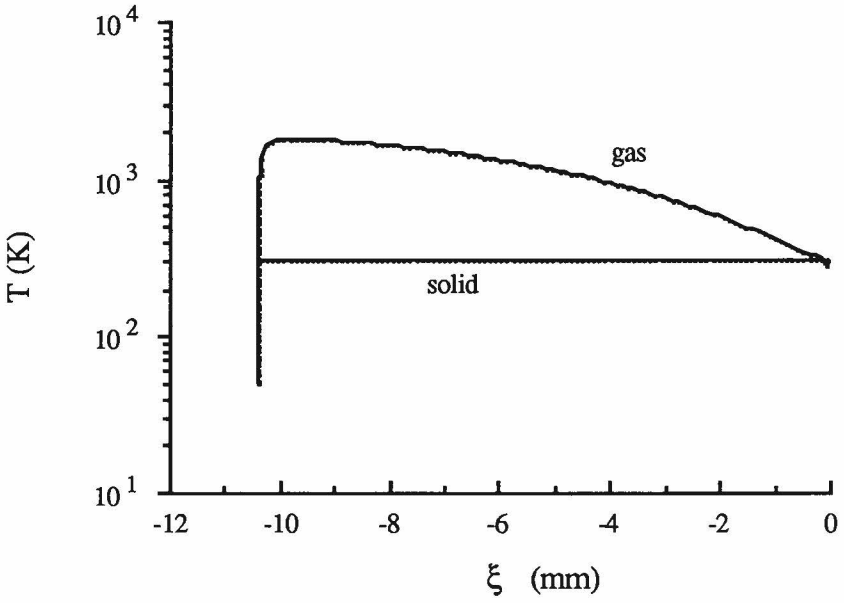

Figure 10 Gas and Solid Temperature Structure, ϕ_{20} = 0.70, D = 100 m/s

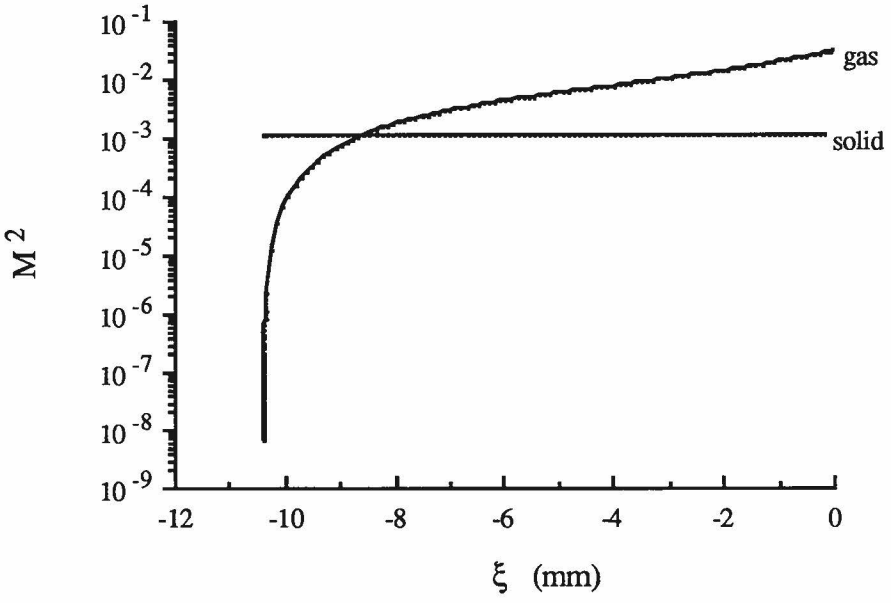

Figure 11 Gas and Solid Mach Number Squared, $\phi_{20} = 0.70$, D = 100 m/s